

Lasers in Manufacturing Conference 2021

Polymer film processing with a high-power industrial femtosecond laser

Chandra Sekher Reddy Nathala^{a,*}, Victor Matylitsky^a, Jim Bovatsek^b

^aMKS Spectra-Physics, Feldgut 9, Rankweil, 6830, Austria

^bMKS Spectra-Physics, 1565 Barber Lane, Milpitas, CA 95035-7409, United States

Abstract

Polymer materials are increasingly important for medical device, flat panel display and microelectronics applications. Due to the high thermal sensitivity of polymers, femtosecond laser processing can minimize heat deposition, and high powers are needed to achieve fast processing. In our work, we present ablation thresholds and cutting speeds for two common polymer materials, polyethylene terephthalate (PET) and polyimide, processed with a 100 W femtosecond laser with single and burst pulses and at infrared and green wavelengths. Cutting speeds were determined for both single-pass and multi-pass strategies. In addition to determining the ablation thresholds and the maximum cutting speed, the processed samples were analyzed for kerf width and heat affected zone (HAZ). With optimized parameters, high speed, high quality cutting of PET and polyimide films was demonstrated with a high-power femtosecond laser.

Keywords: High power femtosecond laser; Femtosecond laser processing; Polymers; High throughput processing

1. Introduction

Polymer materials are increasingly used in various industrial sectors such as medical, automotive, semiconductor, aerospace and display industries. Polyethylene terephthalate (PET) and polyimide (PI) are two such widely used materials. PI film has unique combination of electrical, thermal, chemical and mechanical properties which allow it to withstand extreme temperature, vibration and other demanding environments. PET on the other hand exhibits excellent conformability and high dielectric strength per mil of thickness making it an ideal material for masking applications. Cutting polymer materials with CO₂ laser is well studied [Davim

* Corresponding author. Tel.: +43 5522 82646 .
E-mail address: chandra.nathala@mksinst.com .

et al., 2008, Caiazza et al., 2005, Choudhury et al., 2010]. However, one of the technological problems faced by modern day industry when dealing with polymer materials in general is high precision cutting. Using long pulse lasers or CO₂ laser for cutting of polymer materials results in large kerf widths and large heat affected zones (HAZ). Hence for precision applications, the solution lies in ultrashort lasers. Femtosecond lasers are capable of processing polymer materials with minimum HAZ and, due to high pulse repetition rates, high powers are available to meet demanding throughput requirements. In this work, the effect of pulse number, wavelength, repetition rate and burst mode on ablation thresholds are systematically investigated for two polymer materials: PET and polyimide. Maximum cutting speeds and minimum achievable kerf width as well as HAZ are investigated for various laser and process parameters.

2. Experimental procedure

Two polymer materials, PET and polyimide were irradiated by commercially available industrial femtosecond lasers (MKS Spectra-Physics®). The IR model laser (Spirit® 1030-100) emits pulses of wavelength $\lambda \approx 1030$ nm with maximum pulse energy, $E > 100$ μ J at repetition rates up to 1 MHz, amounting to >100 W of average power for repetition rates of ≥ 1 MHz. The green wavelength laser (Spirit 515-50) emits pulses of wavelength $\lambda \approx 515$ nm with maximum pulse energy, $E > 50$ μ J at repetition rates of up to 1 MHz, amounting to >50 W of average power for repetition rates of ≥ 1 MHz. Pulse duration of both lasers is $t < 400$ fs. The samples, Polyethylene Terephthalate (PET) and Polyimide (PI) used in these experiments are 5 mil (127 μ m) thick and procured from Creative Global Services Inc (Model: CGS-7258 and CGS-5125).

For ablation threshold measurements, the samples were irradiated in stationary mode. Ablation thresholds for number of pulses, $N = 1, 10, 30, 100$ were found for both the IR and green wavelengths. For cutting tests, a 2-axis scanning galvanometer (ScanLAB, intelliSCAN-14) was used. For 1030 nm a f-theta lens of focal length 56 mm was used; and for 515 nm, a telecentric f-theta lens of focal length 100 mm was used. Motorized beam expanders (Sill Optics – Model: S6EZM5076/328 for 1030 nm and model: S6EZM5076/292 for 515 nm) were used to obtain a constant Gaussian beam diameter of $2\omega_0$ ($1/e^2$) ≈ 17.1 μ m for both wavelengths.

3. Ablation Thresholds

When a laser beam is incident on a material surface, the ablation of the material occurs only when the incident laser pulse energy exceeds a minimum value called the ablation threshold. Ablation threshold values depend on several laser and material properties. For a laser beam having a Gaussian spatial distribution, for a given number of pulses (N), and pulse energy E , the ablation crater diameter (D) formed on a material can be related to the ablation threshold, $F_{th}(N)$ [Liu 1982] by

$$D^2 = 2\omega_0^2 \ln\left(\frac{F}{F_{th}(N)}\right) \quad (1)$$

Where ω_0 is the $1/e^2$ gaussian beam radius and F is the peak fluence given by,

$$F = \frac{2E}{\pi\omega_0^2} \quad (2)$$

As can be seen from Eq.(1), the squared ablation crater diameter is logarithmically proportional to the peak laser fluence (F), which is related to the pulse energy E by Eq. (2). This makes it possible to determine the beam radius (ω_0) from a plot of the squared crater diameters (D^2) versus the logarithm of the laser pulse energy E and by extrapolation the threshold pulse energy can be determined. Generally, the ablation threshold decreases with increasing number of pulses. This reduction in threshold can be explained in terms of the incubation model [Jee et al., 1988]. The relation between single-shot threshold fluence $F_{th}(1)$ and N -shot threshold fluence $F_{th}(N)$ has been proposed as given by

$$F_{th}(N) = F_{th}(1)N^{S-1} \quad (3)$$

Where S is called the incubation coefficient characteristic to the accumulation behavior. $S=1$ implies no incubation effect. A more elaborate model of incubation effect is given in [Sun et al., 2015].

3.1. Effect of pulse number

PET and polyimide samples were irradiated with 1, 10, 30, 100 pulses at 1 MHz repetition rate with varying pulse energy at both 1030 nm and 515 nm wavelengths. The irradiated spots were analyzed with an optical microscope, and the crater area and crater diameter were determined for each spot using ImageJ software. The squared crater diameter was plotted against the applied pulse energy for each N and corresponding ω_0 value was determined from the slope of the fitting curves. It has been noticed that for high E and high N , the squared crater diameters do not follow Eq. 1. It is logical to conclude from general theoretical arguments that there could be other mechanisms (excessive heating, etc.) occurring at higher fluences and larger number of pulses. Hence only the data points that follow Eq. 1 were used for the fitting and the corresponding threshold energy values were found by extrapolating the fitting curve to zero crater diameter. The threshold energy value is then converted to threshold fluence using Eq. 3. Fig. 1. (a) & (b) shows the plots of squared crater diameter versus pulse energy when polyimide samples were irradiated with 1030 nm and 515 nm fs laser pulses respectively with various number of pulses $N=1, 10, 30, 100$. Fig. 1. (c) shows the plot of threshold fluence versus N for polyimide sample for IR and green wavelengths. By fitting Eq. 3 to the data points of Fig. 1. (c), the incubation coefficient S was obtained. The errors associated with the threshold fluence values (about 10%) arising from the error in determination of the spot size is not shown in Fig. 1. (c). Fig. 2 shows similar plots for PET sample.

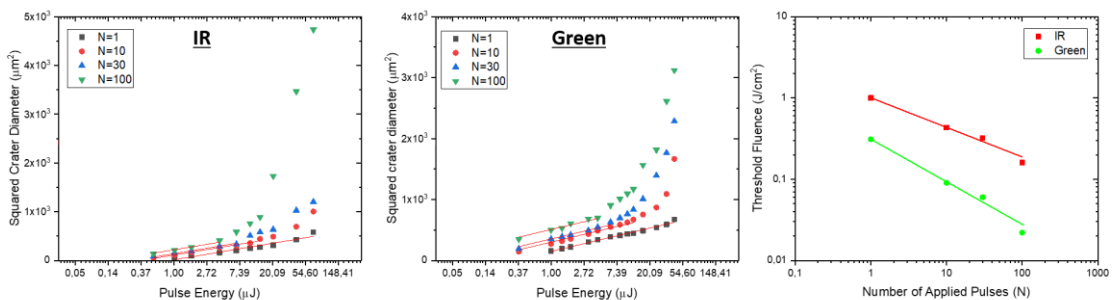


Fig. 1. Plot of squared crater diameters versus the pulse energy for different number of applied laser pulses on a polyimide sample when irradiated with (a) IR (1030 nm) fs laser pulses (b) green (515 nm) fs laser pulses at 1 MHz repetition rate; (c) Plot of threshold fluence versus number of pulses, N of a polyimide sample for IR and green wavelengths with laser running at 1 MHz repetition rate.

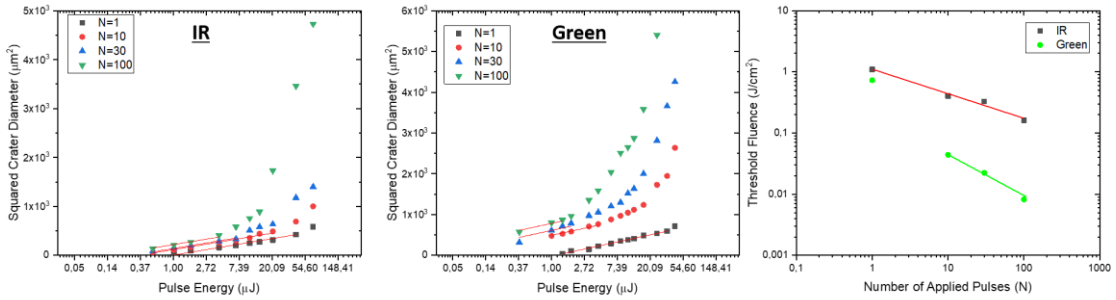


Fig. 2. Plot of squared crater diameters versus the pulse energy for different number of applied laser pulses on a PET sample when irradiated with (a) IR (1030 nm) fs laser pulses (b) green (515 nm) fs laser pulses; (c) Plot of threshold fluence versus number of pulses, N of a PET sample for IR and green wavelengths.

Table 1. Single shot and multi-shot ablation threshold fluence values and incubation coefficients of Polyimide and PET samples for IR and green fs laser pulses

Ablation Threshold Fluence- $F_{th}(N)$ - (J/cm^2)	N=1	N=10	N=30	N=100	Incubation Coefficient (S)
Polyimide- IR	1.00	0.43	0.32	0.16	0.63 ± 0.02
Polyimide - Green	0.31	0.09	0.06	0.022	0.47 ± 0.02
PET - IR	1.09	0.40	0.32	0.16	0.60 ± 0.02
PET - Green	0.73	0.04	0.02	0.008	0.32 ± 0.06

Table 1 lists the single shot and multi-shot ablation threshold fluence values and incubation coefficients of polyimide and PET samples for 1030 and 515 nm femtosecond laser pulses. It can be noticed that for IR wavelengths the ablation threshold values were similar for both polyimide and PET samples. However, with green pulses, the incubation effect is stronger in PET compared to polyimide.

3.2. Effect of repetition rate

For the determination of single shot and multi-shot threshold fluence values, the laser was run at 1 MHz repetition rate. To determine the effect of repetition rate, 30-pulse ablation threshold fluence values was determined for 1 KHz, 10 KHz, 100 KHz, 500 KHz, 1 MHz and 2 MHz repetition rates. Fig. 3 shows the 30-pulse

ablation threshold fluence values at various repetition rates. It can be seen from the plot that the ablation threshold values are constant above the repetition rate of 100 KHz.

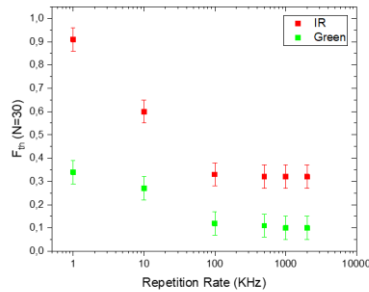


Fig. 3. Threshold Fluence values for 30 pulses versus the repetition rate on a polyimide sample when irradiated with 1030 nm and 515 nm laser pulses

3.3. Effect of burst mode

In burst mode operation, a single high energy laser pulse is divided into several closely spaced, lower energy pulses with the same cumulative energy in the burst envelope as that of the single pulse. To assess the effect of burst mode on processing PET and polyimide samples, single shot threshold fluence values were determined for 2, 3, 5, 7, and 9 burst pulses with 1030 nm femtosecond pulses in polyimide sample. Fig. 4. (a) shows a plot of the squared crater diameters versus pulse energy and Fig. 4. (b) shows the plot of single shot threshold fluence values versus number of burst pulses. It can be seen that the threshold values of burst pulses are higher than that for single pulses.

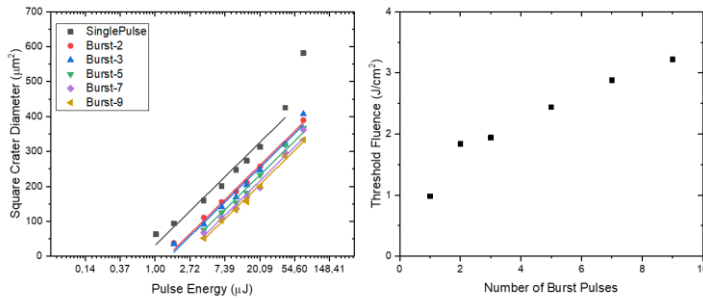


Fig. 4. (a) Plot of squared crater diameters versus the pulse energy for different number of burst pulses on a polyimide sample when irradiated with IR (1030 nm) fs laser pulses at 1 MHz repetition rate; (b) Threshold Fluence values versus the number of burst pulses on a polyimide sample when irradiated with IR (1030 nm) fs laser pulses at 1 MHz repetition rate.

4. Cutting

To determine maximum achievable cutting speeds and minimum achievable kerf widths and HAZ in a 5 mil thick polyimide and PET samples, the samples were cut in single scan and multi-scan modes at 1 MHz and 2

MHz repetition rates with both the IR green lasers. 25 mm long straight-line cuts were made in steps of 10 mm/s and the samples were analyzed to determine the speed at which a through cut was made. Sections 4.1 and 4.2 below show the results of cutting polyimide and PET, respectively.

4.1. Cutting Polyimide

Polyimide samples of 5 mil thickness were cut with single- and multi-scan processes at 1 MHz and 2 MHz. Figures 5 and 6 show microscope images of samples cut with 1030 nm and 515 nm, respectively. Tables 2 and 3 summarize the cutting speeds, kerf widths and HAZ achievable under these conditions.

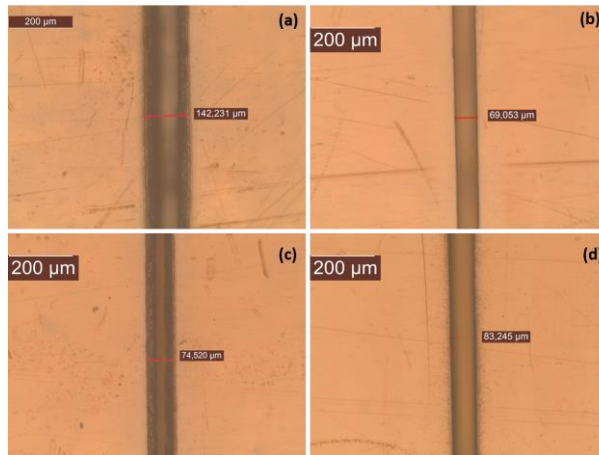


Fig. 5. Optical microscope image of 5 mil thick polyimide sample cut with 1030 nm femtosecond pulses in (a) single scan mode at 1 MHz repetition rate (b) multi-scan mode at 1 MHz repetition rate; (c) single scan mode at 2 MHz repetition rate (d) multi-scan mode at 2 MHz repetition rate.

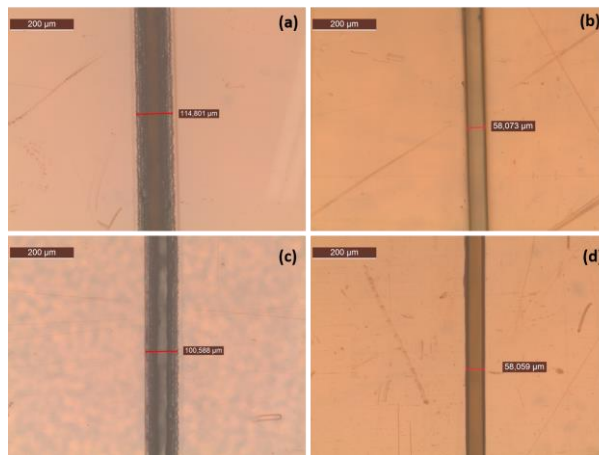


Fig. 6. Optical microscope image of 5 mil thick polyimide sample cut with 515 nm femtosecond pulses in (a) single scan mode at 1 MHz repetition rate (b) multi-scan mode at 1 MHz repetition rate; (c) single scan mode at 2 MHz repetition rate (d) multi-scan mode at 2 MHz repetition rate.

4.2. Cutting PET

PET samples of 5 mil thickness were also cut using single- and multi-scan processes at both 1 MHz and 2 MHz. Fig. 7. shows microscope images of the samples cut with 1030 nm beam and Fig. 8 shows microscope images of samples cut with 515 nm beam. Table 2 and table 3 summarizes the cutting speeds, kerf widths and HAZs achievable under these conditions.

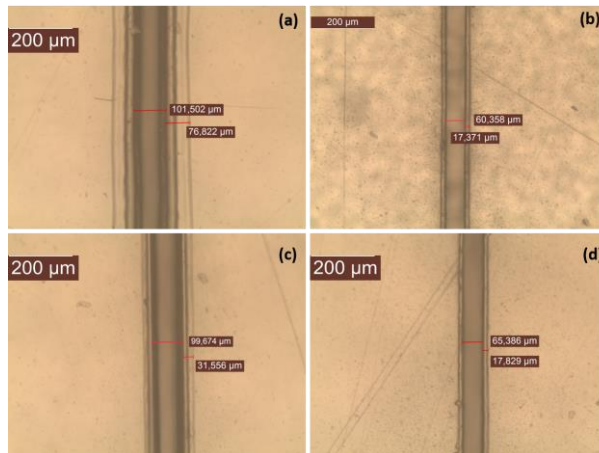


Fig. 7. Optical microscope images of 5 mil thick PET sample cut with 1030 nm femtosecond pulses in (a) single scan mode at 1 MHz repetition rate (b) multi-scan mode at 1 MHz repetition rate; (c) single scan mode at 2 MHz repetition rate (d) multi-scan mode at 2 MHz repetition rate.

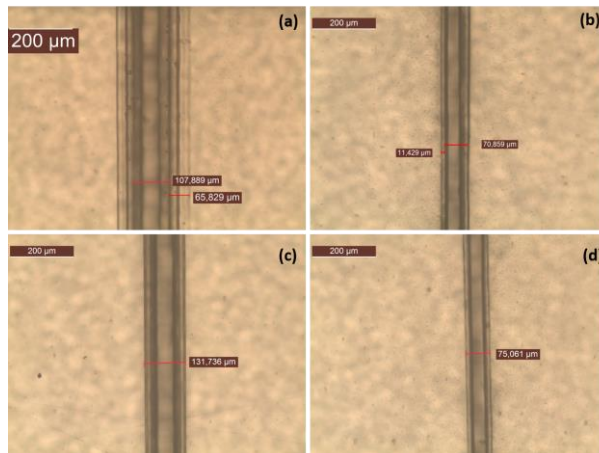


Fig. 8. Optical microscope image of 5 mil thick PET sample cut with 515 nm femtosecond pulses in (a) single scan mode at 1 MHz repetition rate (b) multi-scan mode at 1 MHz repetition rate; (c) single scan mode at 2 MHz repetition rate (d) multi-scan mode at 2 MHz repetition rate.

Table 2. Effective cutting speeds achieved using 70 W of 1030 nm pulses to cut Polyimide and PET films of 5 mil thickness

IR (1030 nm)		1 MHz		2 MHz	
		Single-pass cutting	Multi-pass cutting	Single-pass cutting	Multi-pass cutting
Polyimide	Effective cutting speed (mm/s)	330	250	390	363
	Kerf width (μm)	142	69	74	83
	HAZ (μm)	~10	-	~10	~10
PET	Effective cutting speed	480	400	470	400
	Kerf width (μm)	101	60	99	65
	HAZ (μm)	76	20	31	~18

Table 3. Effective cutting speeds achieved using 42 W of 515 nm pulses to cut Polyimide and PET films of 5 mil thickness

Green (515 nm)		1 MHz		2 MHz	
		Single-pass cutting	Multi-pass cutting	Single-pass cutting	Multi-pass cutting
Polyimide	Effective cutting speed (mm/s)	330	190	420	307
	Kerf width (μm)	114	58	90	58
	HAZ (μm)	~10	-	~10	-
PET	Effective cutting speed	490	333	510	363
	Kerf width (μm)	107	60	93	55
	HAZ (μm)	66	~10	~17	10

From Fig. 5-8 and Table. 2 & 3, it can be seen that the green femtosecond laser with 42 W of average power can cut polyimide and PET films at similar speeds compared to IR beam of 70 W of average power. Moreover, smaller kerf widths and HAZs are achievable with green compared to IR. Hence, operating the green wavelength femtosecond laser with an average power of ~50 W at 2 MHz repetition rate appears to be optimal laser parameters, and a multi-scan processing approach is ideal for cutting (and scribing) these polymer films.

5. Summary and Conclusion

In this paper, the effect of pulse number, wavelength, repetition rate and burst mode on ablation thresholds has been systematically investigated for two important polymer materials: PET and polyimide. Ablation threshold fluence values and incubation coefficients with IR pulses were similar for both samples. However, with green pulses, PET demonstrated higher incubation effect compared to polyimide. For repetition rates above 100 kHz, the ablation threshold values were almost constant and ablation threshold values for burst pulses were higher than single pulse values. For cutting polyimide or PET, highest cutting speeds were achieved in single scan mode, however low kerf widths and HAZs were achieved with green wavelengths in multi-scan mode and at 2 MHz repetition rates. Polyimide sample of 5 mil thick could be cut at > 307 mm/s with 58 μm kerf-width and negligible HAZ. PET could be cut with an effective speed of 363 mm/s with 55 μm kerf width and ~ 10 μm HAZ. These results are applicable for laser processes in medical device, flat panel display and microelectronics.

References

- Davim, J. & Barricas., Nuno & Conceição., Marta & Carlos., Oliveira., 2008. Some experimental studies on CO₂ laser cutting quality of polymeric materials. *Journal of Materials Processing Technology - J MATER PROCESS TECHNOL.* 198. 99-104.
- F. Caiazzo., F. Curcio., G. Daurelio., F. Memola Capece Minutolo., 2005. "Laser cutting of different polymeric plastics (PE, PP and PC) by a CO₂ laser beam"., *Journal of Materials Processing Technology.*, Volume 159, Issue 3., Pages 279-285.
- I.A. Choudhury., S. Shirley., 2010. "Laser cutting of polymeric materials: An experimental investigation" *Optics & Laser Technology*; Volume 42, Issue 3, Pages 503-508.
- J. Liu, 1982. "Simple technique for measurements of pulsed Gaussian-beam spot sizes," *Opt. Lett.* 7, 196-198.
- Y. Jee., M. Becker., and R. Walser., 1988. "Laser-induced damage on single-crystal metal surfaces," *J. Opt. Soc. Am. B* 5, 648-659 (1988).
- Zhanliang Sun., Matthias Lenzner., and Wolfgang Rudolph., 2015. "Generic incubation law for laser damage and ablation thresholds", *Journal of Applied Physics* 117, 073102.